

Optimization of The Use of Energy-Weighted AVO Attributes to Identify Hydrocarbon

* NOOR FAUZI ISNIARNO, ¹ DONO GUNTORO,
¹ WAHYU BUDHI KHORNIAWAN, ² ASHARI ARIES

*,¹ Universitas Islam Bandung, Bandung, Indonesia

² Institut Teknologi Bandung, Bandung, Indonesia

Correspondance author: noorfauzi@unisba.ac.id *

Article

Article History

Received: 14/07/2022

Reviewed: 18/01/2023

Accepted: 30/01/2023

Published: 30/01/2023

DOI:

doi.org/10.29313/ethos.v11i1.10179



This work is licensed under a Creative Commons Attribution 4.0 International License

Volume : 11
No. : 1
Month : January
Year : 2023
Pages : 34-44

Abstract

Amplitude Variation with Offset (AVO) is a technique that is often used as an indicator of the presence of hydrocarbons in seismic data. This technique uses a mathematical approximation of the Zoeppritz equation to determine the change in amplitude as a function of the angle of incidence and relates it to the rock properties and fluid content within it. The energy AVO attribute weight is very effective in identifying the presence of hydrocarbon. This is because the energy weighted AVO attribute, in principle, amplifies an anomalous response related to the presence of hydrocarbons and reduces seismic around the anomaly. The advantage of this attribute is its ability to distinguish the response of hydrocarbon anomalies to other anomalies caused by lithology such as coal. In addition, this attribute is applicable to pre-stack and post-stack seismic data.

Keywords: AVO; Hydrocarbon; Post-stack; Pre-stack; Seismic energy.

© 2023 Ethos : Jurnal Penelitian dan Pengabdian Kepada Masyarakat, Unisba Press. All rights reserved.

Introduction

The global demand for oil and gas hydrocarbons is still very high (1). This is consistent with technological advances and human life civilization which is still very dependent on oil and gas as the main resource (5). The need for fuels that depend on oil and gas, increases every year (6). On the other hand, the discovery of oil and natural gas is becoming increasingly challenging and the reserves are diminishing, making exploration and exploitation more difficult (7). This is because the existing wells are old, the technology used is outdated and other influencing factors make the presence of oil and gas increasingly difficult (8).

The increase in petroleum needs is not matched with the increase in production causing Indonesia to be threatened with an energy crisis (2). The oil reserves declining are caused by two main factors, namely oil exploitation and the lack of exploration or geological surveys to find new oil reserves (9). One of the actions that can be taken to support the availability of oil and gas resources is to carry out oil and gas exploration activities including reservoir characterization to find a new work area using appropriate methods

and technology (10).

Geophysics is a part of natural science which is a combination of geology and physics (11). In a broad sense, geophysics is providing tools and data to study the structure and composition of the Earth's interior (3). Geophysical exploration techniques are part of a relatively new technological field (12). The rapid development of computer technology has made it easier to collect data and analyze data in geophysical exploration (13). The method in geophysical engineering that is often used in oil and gas exploration is the seismic method (14). Seismic is a hydrocarbon exploration method that uses the principle of wave propagation (15). However, at the implementation stage, this technology is very expensive and onerous technology. So that any data generated must be optimized in depth (16).

Therefore, a new breakthrough is needed in the science of geophysical exploration in searching for the presence of hydrocarbons (4). This breakthrough is expected to be a more practical and cheaper solution in order to reduce the increasing exploration time and operational costs (17). In geophysical engineering, the science that is experiencing rapid development is seismic attributes (18). The Amplitude Versus Offset (AVO) method is a method that observes variations in the amplitude of the P wave for the appearance of bright spots or dim spots on seismic sections (19). Seismic attributes are all forms of information that are derived from seismic data either through computation or direct measurement (20). This seismic attribute is needed to clarify the presence of an anomaly that is invisible when seen in ordinary seismic data (21).

Energy-weighted AVO is a new seismic attribute obtained from the Zoeppritz equation approach. The main principle is to increase the seismic response of sandstones that contain gaseous hydrocarbons to the surrounding seismic background. In addition, this attribute can distinguish the response of hydrocarbon anomalies from anomalies caused by other things such as coal. What's more interesting is that this attribute can be applied to pre-stack and post-stack seismic data.

Research Method

The study area, the Penobscot Field, is located to the southeast of the Canadian province of Nova Scotia and to the northwest of the island of Sable. The field area of the survey area is 86.62 km². Significant hydrocarbon discoveries on the Scotia Shelf are located in the Sable subbasin in the vicinity of the Sable Islands. The Penobscot field is located in an up-dip geopressure area as well as the Cohasset and Panuke fields. All of these fields have abundant oil reserves in the Logan Canyon Formation and Upper Mississauga. Meanwhile, the presence of oil and gas in the Penobscot field is near the Middle Mississauga Formation. The main hydrocarbon deposit in the Sable subbasin is located in a downdip section to the southeast of the Penobscot field. The first prospect is located on the edge of the Abenaki carbonate shelf, west of the main source of clastic sediments. The edges of this shelf are more sloping like in the Cohasset area, dominated by sandstone, shale, and limestone.

AVO is a concept based on changes in the amplitude of the reflected seismic signal as the distance from the source to the receiver or offset increases. The amplitude at a small offset differs from the amplitude at a large offset and the offset distance is related to the angle of incidence of the waves. As the offset increases, so does the angle of incidence. Therefore, this concept is usually referred to as Amplitude Variation with Angle (AVA).

This concept was first discovered by Zoeppritz who showed the relationship between the reflected and transmitted P and S wave amplitudes with the incident wave angle that is not equal to zero. The angles of the incident reflected, and transmitted waves follow Snell's law.

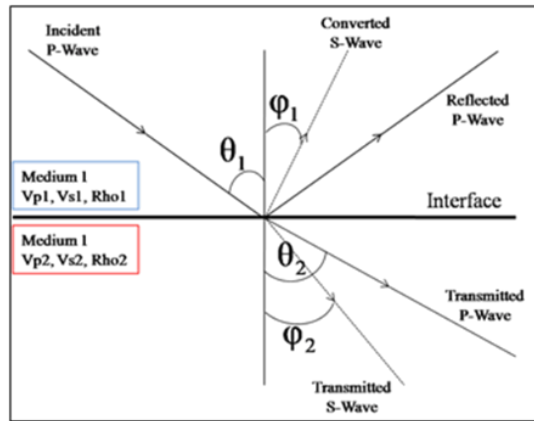


Figure 1. Schematic of wave propagation when it crosses the boundary between two media

The amplitude, angle of reflection, and transmission of P and S waves depend on the angle of incidence and the physical properties of the two media through which the waves pass. Zoeppritz describes it mathematically in the following equation:

$$\begin{bmatrix} R_p(\theta_i) \\ R_s(\theta_i) \\ T_p(\theta_i) \\ T_s(\theta_i) \end{bmatrix} = \begin{bmatrix} -\sin \theta_1 & -\cos \phi_1 & \sin \theta_2 & \cos \phi_2 \\ \cos \phi_1 & -\sin \phi_1 & \cos \theta_2 & -\sin \phi_2 \\ \sin 2\theta_1 & \frac{V_{p1}}{V_{s1}} \cos 2\phi_1 & \frac{\rho_2 V_{s2}^2 V_{p1}}{\rho_1 V_{s1}^2 V_{p2}} \cos 2\phi_1 & \frac{\rho_2 V_{s2}^2 V_{p1}}{\rho_1 V_{s1}^2 V_{p2}} \cos 2\phi_2 \\ \cos 2\theta_1 & \frac{V_{s1}}{V_{p1}} \cos 2\phi_1 & \frac{\rho_2 V_{p2}}{\rho_1 V_{p1}} \cos 2\phi_1 & -\frac{\rho_2 V_{s2}}{\rho_1 V_{p1}} \cos 2\phi_2 \end{bmatrix}^{-1} \begin{bmatrix} \sin \theta_1 \\ \cos \theta_1 \\ \sin 2\theta_1 \\ \cos 2\phi_1 \end{bmatrix}$$

However, the weakness of the Zoeppritz equation is that it does not show an easy understanding of the relationship between changes in the amplitude and variations in the physical properties of the medium through which it passes. Therefore, a number of Zoeppritz equation approaches have been carried out by several experts. The equation is written by separating three factors, namely the speed of the P wave, the speed of the S wave, and the density. Mathematically, the equation of Aki and Richards is:

$$R(\theta) = a \frac{\Delta V_p}{V_p} + b \frac{\Delta \rho}{\rho} + c \frac{\Delta V_s}{V_s}$$

Ostrander demonstrated the seismic response in a layer model of shale-gas-sands with smaller acoustic impedance properties of sandstones than shales. According to him, the change in the amplitude of the seismic reflection to the increase in offset is directly related to the change in Poisson's ratio.

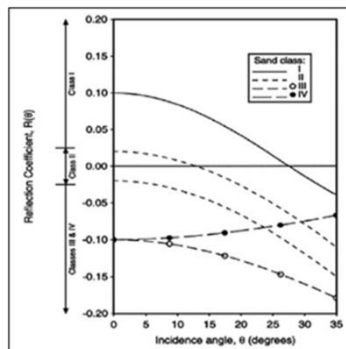


Figure 2. Classification of AVO classes by Rutherford and Williams

Several years later, Rutherford and Williams (1989) carried out a further classification and divided them into three classes namely: 1) AVO class 1, the large positive amplitude intercept value at the near offset decreases with increasing offset. Even at the far offset, there is a polarity reversal to be negative. The gradient value is negative and larger than AVO class 2 and 3. This anomaly is usually found in onshore areas with gas-sand areas that are quite hard, old, and have experienced high compaction; 2) AVO class 2, the small intercept values at near offsets and the small gradients with negative values. If the intercept price is positive, then it is called class 2p. P means there is a polarity reversal at the far offset. Meanwhile, if the intercept price is negative, then it is called AVO class 2, without any polarity reversal at the far offset. This class 2 AVO anomaly has a very small (near zero) impedance contrast between the gas-sand and the overlying rock (usually shale). Generally, this anomaly is found in moderately compacted gas-sand; 3) AVO class 3, large negative intercept values at near offsets and increasingly negative with increasing offsets. The impedance value of the gas-sand is smaller than the cover rock. This anomaly is very easy to recognize on a seismic section known as a bright spot. Gas-sand in this class has less compacted properties.

Results & Discussion

The most significant thing is the loss of the seismic background so that the gas-sands anomaly response remains. For classes 1 and 2 there is a slight attenuation on the top and base. Especially for class 1, the amplitudes at the top and base are collected at different offsets making it difficult to detect on the stack section. For class 2, the amplitude is relatively small so it is also difficult to detect on the stack section.

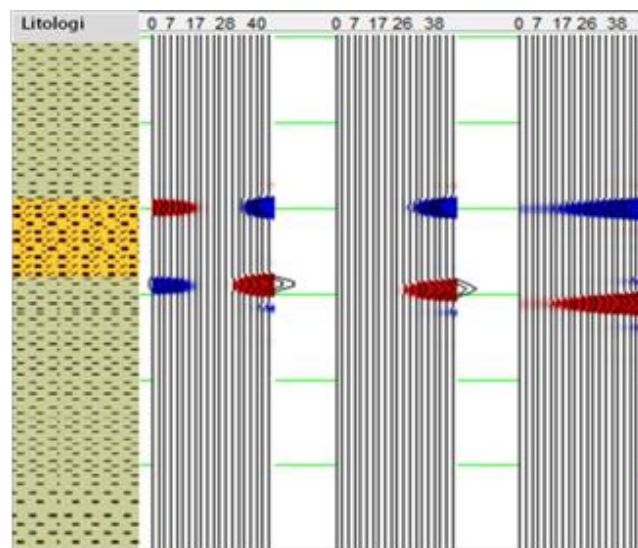


Figure 3. Synthetic CDP gathers in the form of class 1, 2, and 3 AVO responses (left to right) after the EAVO attribute was applied. The order of lithology from top to bottom is shale-gas-sandstone-shale. Trough blue and peak red

For class 3, the amplitude is relatively much larger than the class 2 response. It can be seen that the class 3 response experiences increased energy weighting as the angle increases. The top and base are easy to detect on the stack section. The class 3 AVO anomaly response is similar to the coal anomaly response at the ordinary gather section. Therefore, energy weighting is carried out on the two anomalies and see the resulting differences. Figure 4a shows the response of AVO class 3 which is experiencing weighted energy, while Figure 4b shows the response of coal anomaly after applying the EAVO attribute. It's just that, at both gathers, the seismic background or what could be considered noise is attenuated. This is an advantage of this attribute because it can distinguish between class 3

AVO anomaly responses and coal which in ordinary gather cross-sections these two responses are similar.

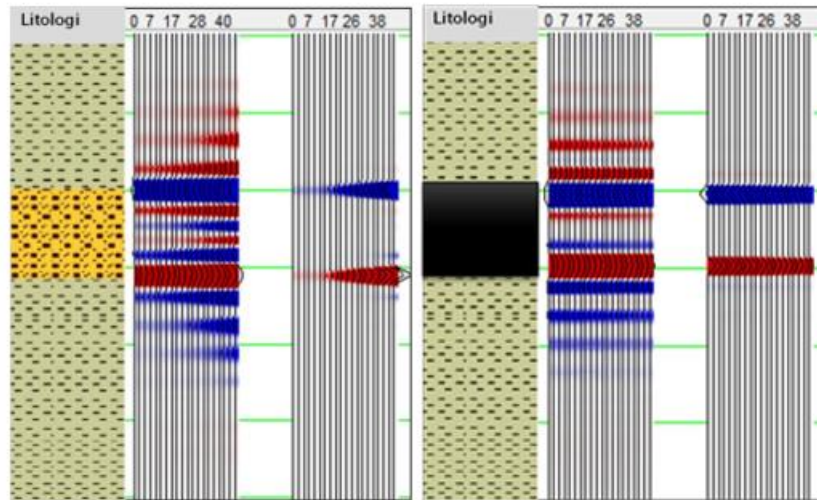


Figure 4. a) AVO class 3 synthetic model (left) and response after weighting energy (right).
 (b) Coal model (left) and response after weighting energy (right)

This analysis needs to be done to find out the effective range of angles for using this attribute. Figure V.3 shows the relationship curve between the amplitude change response of the class 3 AVO model after weighting energy and the angular range. The class 3 AVO model was chosen because this attribute is unique only for class 3 AVO. From the curve, it can be seen that the amplitude change is not significant in the narrow-angle range of 20°. Significant amplitude changes can be seen at a wide angle range, which is around 30-40°. The figure shows that this attribute depends on a wide angle range of seismic data to provide optimal results.

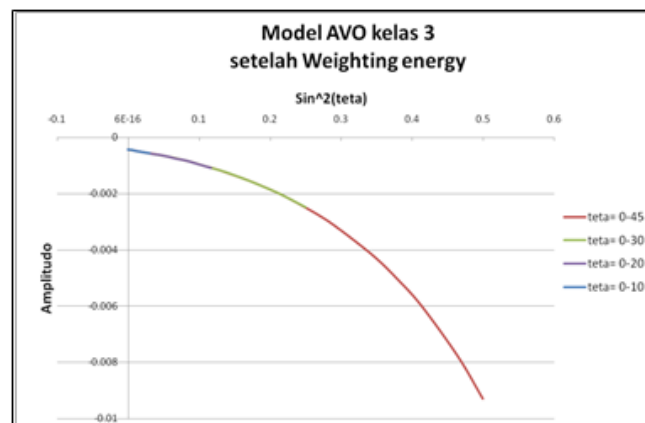


Figure 5. The range angle effectiveness analysis curve on the EAVO attribute

Checking the available geological data is an important thing. In addition, good data information is very important, especially those which related to rock sample experiments. Everything that indicates the presence of hydrocarbons is the main focus of this study. As it is known from the log data that there are eight layers of sandstone (sand 1, 2, 3, 3A, 4, 5, 6, and 7). This sandstone layer is found in the Middle Mississauga Formation. In addition, the RFT (Repeat Formation Tester) test showed that some of the samples taken from the sandstone layer contained hydrocarbons.

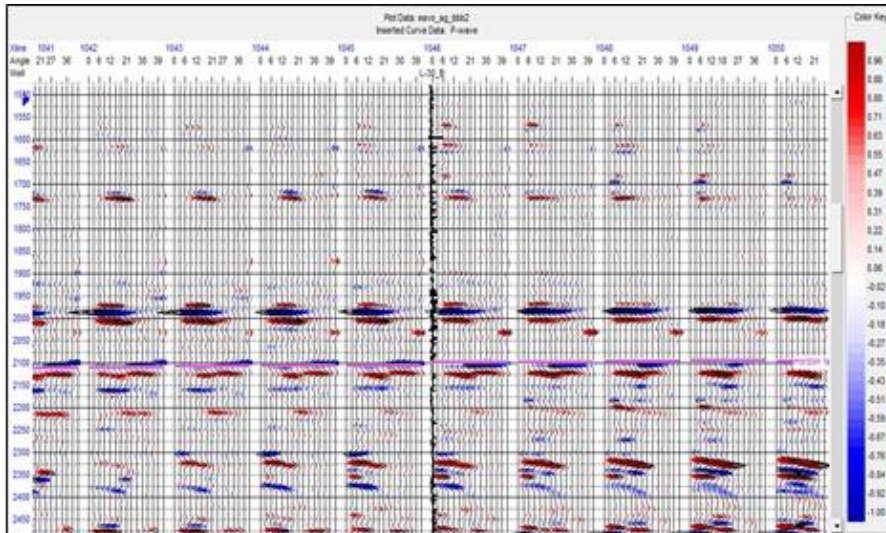


Figure 6. Angle gathers the seismic section on inline 1284 around the location of the L-30 well after applying the EAVO attribute. The angle range is 0-43°

In Figure 6, it can be seen that most of the seismic background can be attenuated compared to the previous Figure. Figure 7 clarifies the appearance of one of the CDPs from Figure V.4. It can be seen that at around 1980 ms, it does not show any particular AVO anomaly response. Whereas at 2100 ms, the seismic response showed a similar response to class 3 AVO. According to the well-seismic-tie results, the target zone at 2100 ms fit with marker sand #4. The presence of these hydrocarbons can be correlated with the results of the RFT (Repeat Formation Tester) tests on rock samples in this zone. According to Table V.1, the sample in sand #4 contains 3800 cc of condensate and 10 cf of gas.

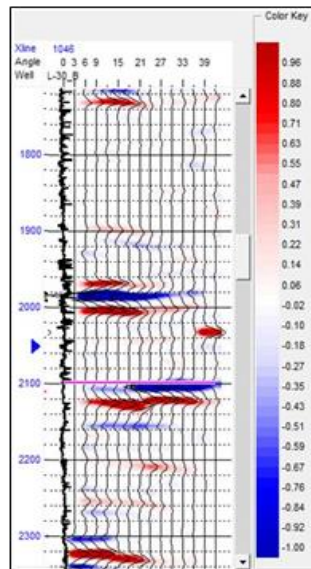


Figure 7. Angle gathers seismic cross-section at one of the CDPs in well L-30 location after applying the EAVO attribute

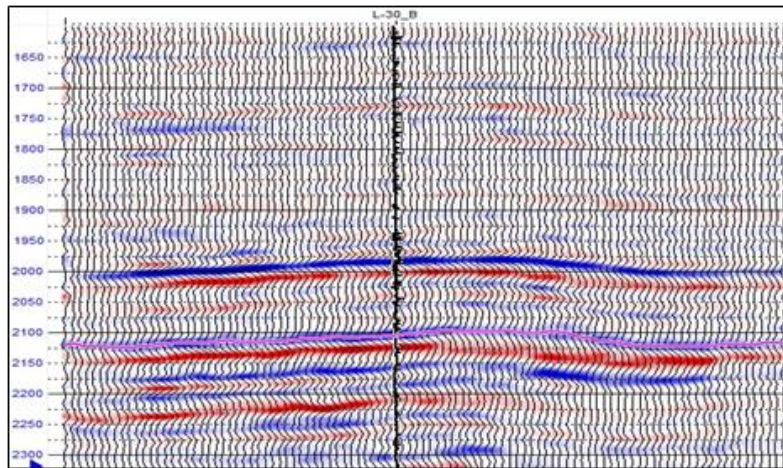


Figure 8. Angle gathers seismic cross-section after stacking

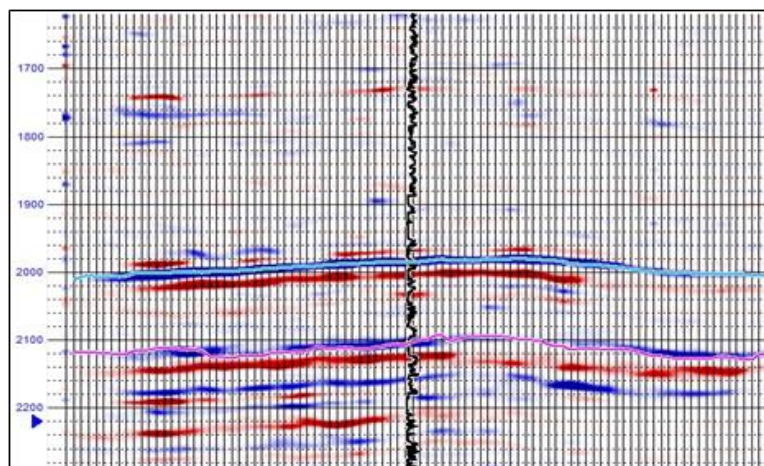


Figure 9. Cross section of the seismic gather stack that has been applied the EAVO attribute

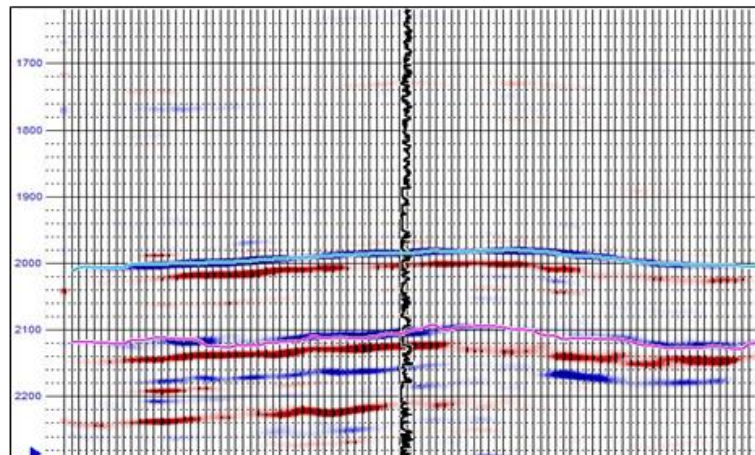


Figure 10. Seismic cross section by directly applying the EAVO attribute to the post-stack data

Then we have a cross-section of the stack from the regular CDP gather (Figure 8) and from the CDP gather that has been applied with EAVO (Figure 9). It appears that the remaining gas-containing sands layer is in the purple horizon, otherwise, it is attenuated. In addition, if this attribute is applied directly to the regular stack section, (Figure 10), the same response appears on the stack section from the CDP gather after EAVO. This is clearly seen from the difference between these two sections (Figure 11).

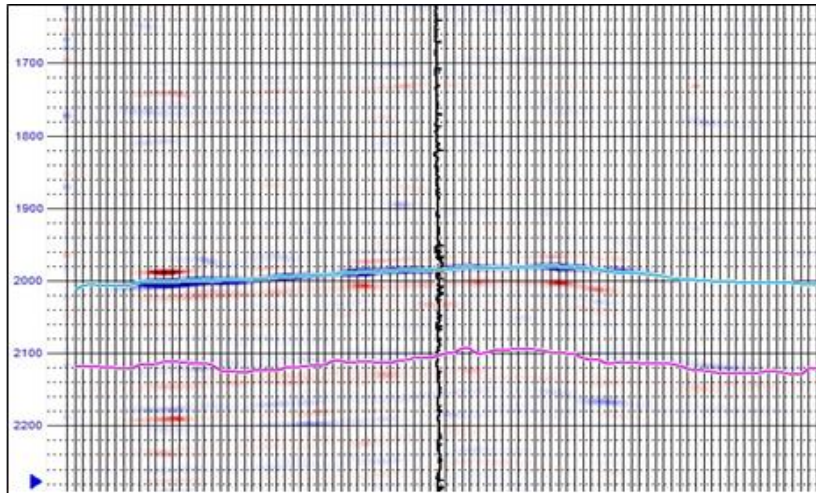


Figure 11. The difference between the two previous sections

The interesting thing about this attribute can be seen in Figure 12 which shows the difference in amplitude response of the seismic section before and after the EAVO attribute was applied. As seen in Figure 12 to the left, the circled portion shows a relatively constant amplitude response along the target region (purple horizon). Whereas in Figure 12 on the right, the amplitude response in the circled part gradually disappears (drops) relative to the surrounding anomalies. The missing portion in Figure 12 on the right can then be interpreted as the absence of a class 3 hydrocarbon or AVO gas response.

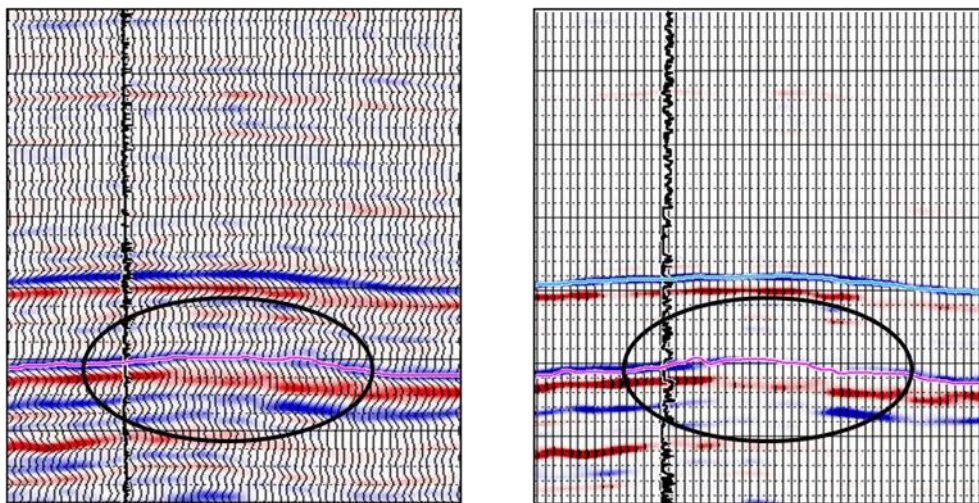


Figure 12. A comparison of hydrocarbon detection on seismic sections before (left) and after (right) the EAVO attribute was applied

In fact, this attribute is working on both pre-stack and post-stack data. This is in line with what is shown in Equations (III.13) and (III.18). This attribute is then compared to the conventional AVO attribute, namely the product attribute ($A*B$). The results still show the same response, especially in class 3 gas-sand AVO (Figure 13).

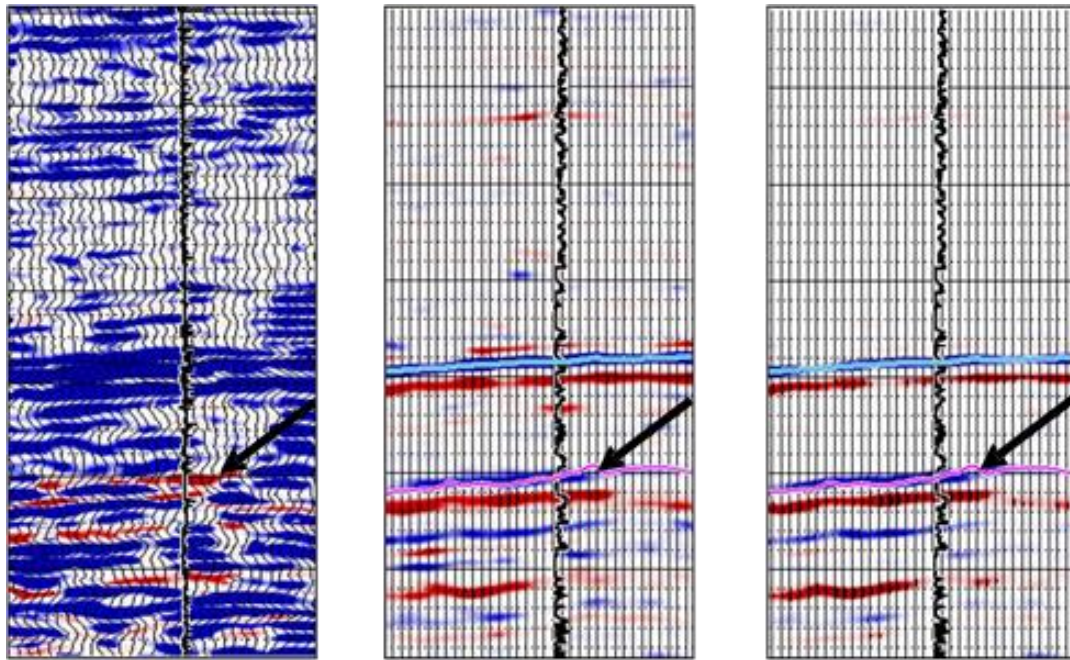


Figure 13. Product attributes ($A*B$) (left), EAVO attributes from pre-stack data (middle), and post-stack data (right) show an anomalous response to the same gas-sand (shown by arrows)

Conclusions

The Energy-Weighted Amplitude Versus Offset (EAVO) attribute can identify the presence of hydrocarbons at a depth of about 2639 m or at a time of 2100 ms. The Energy-Weighted Amplitude Versus Offset (EAVO) attribute succeeded in identifying the presence of class 3 Amplitude Versus Offset (AVO) gas, which when compared with the AVO Product attribute, does not cause differences in interpretation. The Energy-Weighted Amplitude Versus Offset (EAVO) attribute can reduce the ambiguity of the AVO anomaly in pre-stack data by being able to distinguish Class 3 Amplitude Versus Offset (AVO) anomalies from other classes, including anomalies from coal. The Energy-Weighted Amplitude Versus Offset (EAVO) attribute provides the same response for both pre-stack and post-stack seismic data. Implementing and utilizing the Energy-Weighted Amplitude Versus Offset (EAVO) attribute is both fast and simple.

References

- Isniarno,NF.,Nurfajar,IR.,Saputra, MO. 2021. Analisis Discounted Cash Flow (Dcf) Dalam Investasi Tambang Dan Kelayakan Ekonomi Pada Ekstraksi Timah Dengan Menggunakan Teknologi Klorinasi Basah. *Ethos: Jurnal Penelitian dan Pengabdian Masyarakat*, Vol 9, No.1, Januari 2021: 112-117. <https://doi.org/10.29313/ethos.v9i1.6626>
- Isniarno,NF., Alfarel,MR.,Gumelar,BB., 2022. Optimasi Iterasi Dan Root Means Square (Rms) Dalam Penentuan Batas Litologi Dari Vertikal Elektrical Sounding (Ves). *Ethos: Jurnal Penelitian dan Pengabdian kepada Masyarakat*, Vol 8, No.1, Juni 2019: 41-48. <https://doi.org/10.29313/ethos.v8i1.5058>
- Isniarno, NF., Azis, G., Iswandaru. 2020. Hydrological monitoring in open PIT mining areas using geodatabase attribute in Geographic Information Systems (GIS). *IOP Conf. Series: Materials Science and Engineering* 830 (2020) 042043. doi:10.1088/1757-899X/830/4/042043.
- Isniarno,NF., Amukti, R., Nurhasan, R. 2020. Analysis of velocity groundwater in unconfines aquifer zone using infiltration measurement. *IOP Conf. Series: Materials Science and Engineering* 830 (2020) 042047. doi:10.1088/1757-899X/830/4/042047.

- Fadul, M. F., El Dawi, M. G., & Abdel-Fattah, M. I. (2020). Seismic interpretation and tectonic regime of Sudanese Rift System: Implications for hydrocarbon exploration in neem field (Muglad Basin). *Journal of Petroleum Science and Engineering*, 107223. doi:10.1016/j.petrol.2020.107223.
- Mark, N. J., Schofield, N., Pugliese, S., Watson, D., Holford, S., Muirhead, D., ... Healy, D. (2018). Igneous intrusions in the Faroe Shetland basin and their implications for hydrocarbon exploration; new insights from well and seismic data. *Marine and Petroleum Geology*, 92, 733–753. doi:10.1016/j.marpetgeo.2017.12.005 .
- Chen, Z., Qiu, L., & Liu, Y. (2021). Pre-salt regional structure and its control for hydrocarbon accumulation in Lower Congo Basin from seismic and gravity data. *Journal of Applied Geophysics*, 188, 104312. doi:10.1016/j.jappgeo.2021.104312.
- Bredesen, K., Rasmussen, R., Mathiesen, A., & Nielsen, L. H. (2021). Seismic amplitude analysis and rock physics modeling of a geothermal sandstone reservoir in the southern part of the Danish Basin. *Geothermics*, 89, 101974. doi:10.1016/j.geothermics.2020.101974.
- Goulart, J. P. de M., & de Castro, D. L. (2020). Models of hydrocarbon traps associated with gas chimney in Parnaíba Basin (NE Brazil). *Journal of South American Earth Sciences*, 102908. doi:10.1016/j.jsames.2020.102908.
- Singh, A., & Rao, G. S. (2021). Crustal structure and subsidence history of the Mannar basin through potential field modelling and backstripping analysis: Implications on basin evolution and hydrocarbon exploration. *Journal of Petroleum Science and Engineering*, 206, 109000. doi:10.1016/j.petrol.2021.109000.
- Luan, X., Islam, M. S., Wei, X., Lu, Y., Fan, G., Pau, S. K., & Lwin, S. M. (2021). Hydrocarbon accumulation in an active accretionary prism, a case study in the deepwater Rakhine Basin, Myanmar offshore. *Journal of Asian Earth Sciences*, 221, 104941. doi:10.1016/j.jseaes.2021.104941
- Ye, T., Chen, A., Hou, M., Niu, C., & Wang, Q. (2021). Characteristic of the Bodong segment of the Tanlu Fault Zone, Bohai sea area, eastern China: Implications for hydrocarbon exploration and regional tectonic evolution. *Journal of Petroleum Science and Engineering*, 201, 108478. doi:10.1016/j.petrol.2021.108478
- Radwan, A. E., Rohais, S., & Chiarella, D. (2021). Combined stratigraphic-structural play characterization in hydrocarbon exploration: A case study of Middle Miocene sandstones, Gulf of Suez basin, Egypt. *Journal of Asian Earth Sciences*, 218, 104686. doi:10.1016/j.jseaes.2021.104686
- Mahdavi, A., Roshandel Kahoo, A., Radad, M., & Soleimani Monfared, M. (2021). Application of the local maximum synchrosqueezing transform for seismic data. *Digital Signal Processing*, 110, 102934. doi:10.1016/j.dsp.2020.102934.
- Ogbe, O. B., Okoro, A. U., Ogagarue, D. O., Osokpor, J., Overare, B., Ocheli, A., ... Oluwajana, O. A. (2021). Reservoir hydrocarbon prospectivity and productivity evaluations of sands S-600 and S-700 of Fega field, onshore Niger Delta Basin, Nigeria. *Journal of African Earth Sciences*, 184, 104311. doi:10.1016/j.jafrearsci.2021.104311.
- Wang, D., Gao, Y., Tong, P., Wang, J., Yao, C., & Wang, B. (2021). Electroseismic and seismoelectric responses at irregular interfaces: Possible application to reservoir exploration. *Journal of Petroleum Science and Engineering*, 202, 108513. <https://doi.org/10.1016/j.petrol.2021.108513>.
- Guo, Q., Ba, J., Luo, C., & Pang, M. (2021). Seismic rock physics inversion with varying pore aspect ratio in tight sandstone reservoirs. *Journal of Petroleum Science and Engineering*, 207, 109131. doi:10.1016/j.petrol.2021.109131
- Tan, M., Zhu, X., Wei, W., & Pan, R. (2021). Characteristics and implications of Albian volcanism in a magma-rich rift basin: Seismic volcano stratigraphic and geomorphological evidence from the Upper Suhongtu Member in the Chagan Sag, China-Mongolia border region. *Marine and Petroleum Geology*, 131, 105164. doi:10.1016/j.marpetgeo.2021.105164

- Larki, E., Tanha, A. A., Parizad, A., Soltani Soulgani, B., & Bagheri, H. (2021). Investigation of quality factor frequency content in vertical seismic profile for gas reservoirs. *Petroleum Research*, 6(1), 57–65. doi:10.1016/j.ptlrs.2020.10.002
- Ghoneimi, A., Farag, A. E., Bakry, A., & Nabih, M. (2021). A new deeper channel system predicted using seismic attributes in scarab gas field, west delta deep marine concession, Egypt. *Journal of African Earth Sciences*, 177, 104155. doi:10.1016/j.jafrearsci.2021.104155
- Usman, M., Siddiqui, N. A., Garzanti, E., Jamil, M., Imran, Q. S., & Ahmed, L. (2021). 3-D seismic interpretation of stratigraphic and structural features in the Upper Jurassic to Lower Cretaceous sequence of the Gullfaks Field, Norwegian North Sea: A case study of reservoir development. *Energy Geoscience*, 2(4), 287–297. doi:10.1016/j.engeos.2021.06.001.